A&A, 690, A157 (2024)
https://doi.org/10.1051/0004-6361/202451036

Astronomy & Astrophysics

HII galaxies as standard candles: Evolutionary corrections*

Jorge Melnick[1,2,**] and Eduardo Telles[2]

[1] European Southern Observatory, Av. Alonso de Cordova, 3107 Santiago, Chile
e-mail: jmelnick@eso.org
[2] Observatorio Nacional, Rua José Cristino 77, 20921-400 Rio de Janeiro, Brazil

Received 7 June 2024 / Accepted 25 July 2024

ABSTRACT

Over the past decade, the relation between the Balmer-line luminosity of HII galaxies and the velocity width of the emission lines, the $L - \sigma$ relation, has been painstakingly calibrated as a cosmological distance indicator with seemingly spectacular results: the Hubble constant and the energy density of dark energy obtained using the $L - \sigma$ indicator agree remarkably well with the values from canonical indicators. Since most of the luminosity of these young compact starburst galaxies is emitted by a few narrow emission lines, they can be observed with good precision up to redshifts of $z \sim 7$ with JWST, making the $L - \sigma$ indicator a potentially unique cosmological probe. However, the precision of the method remains too low to effectively constrain the relevant cosmological parameters, notably the equation of state of dark energy. The scatter of the $L - \sigma$ relation is significantly larger than the random observational errors, so we do not have a good handle on the systematics of the method. In a previous paper, we posited that since the ionizing radiation of these young galaxies fades rapidly over timescales of only a few million years, age differences could be the main underlying cause of the scatter. In this paper, we explore several different ways of explaining the scatter of the correlation, but without success. We show that the majority of HII galaxies are powered by multiple starbursts of slightly different ages, and therefore that the equivalent widths are not reliable chronometers to correct the luminosities for evolution. Thus, it is not likely that the accuracy of the $L - \sigma$ distance indicator can be improved in the near future. Since we do not fully understand either the systematics or the underlying physics of the $L - \sigma$ relation, using large samples of distant HII galaxies may or may not improve the accuracy of the method.

Key words. galaxies: ISM – galaxies: kinematics and dynamics – galaxies: starburst – distance scale

1. Introduction

HII galaxies are dwarf compact galaxies whose luminosities are dominated by one or more young starburst components. A significant fraction of their luminosity is emitted in a few strong and narrow emission lines that make HII galaxies relatively easy to observe out to redshifts of cosmological relevance. HII galaxies exhibit a correlation between the luminosity of the Balmer emission lines (typically Hβ; L(Hβ)) and the width of these lines and the stronger [OIII] lines. This correlation (the $L - \sigma$ relation) has been calibrated as a distance indicator using Giant HII Regions in local late-type galaxies with accurately measured distances to define the zero point (González-Morán et al. 2021 and references therein).

The main advantage of the $L - \sigma$ distance indicator is that it can be applied to galaxies out to $z \sim 7$ (Chávez et al. 2024); The main drawback is that the scatter of the relation is not only substantially larger than the observational errors, but also not well understood. We really do not have a good handle on the systematic errors associated with the cosmological parameters derived using HII galaxies, therefore, which may be quite significant given that the dispersion of distance moduli for high-z galaxies derived from $L - \sigma$ is of several magnitudes (González-Morán et al. 2021; Chávez et al. 2024).

Although the ages of the starburst clusters that power HII galaxies are selected to be shorter than a few million years (Myr), in this short age span the ionizing radiation emitted by these clusters evolve significantly. So from this evolution alone we expect a scatter at least similar, if not larger, than that observed.

In our study of 2234 high-excitation HII galaxies from the Sloan Digital Sky Survey (SDSS), we showed that the scatter in the relation between the Hβ luminosity and the mass of the ionizing (starburst) cluster determined from spectral energy distribution (SED) models correlates very well with the equivalent width of Hβ (EW(Hβ)) expected from *Starburst99* models (Telles & Melnick 2018). Galaxies with equivalent widths larger than the average of the sample are systematically above the regression line, and vice versa.

The same result does not obtain in the sample of low-redshift HII galaxies used in the calibration of the $L - \sigma$ relation (Melnick et al. 2017). We suggested in that paper that the problem could be due to contamination of the continuum by evolved (old and intermediate-age) stars through the EW(Hβ). In this paper, we explore that idea, using SED population synthesis models to disentangle the effect of evolved stars.

2. The $L - \sigma$ relation revisited

In Melnick et al. (2017), we explored the scatter of the relation using new velocity dispersions determined from the [OIII]5007 lines rather than the traditional Hβ and photometric data from the SDSS instead of the ad hoc wide-aperture spectrophotometry from Chávez et al. (2014). The rationale behind these choices, as is explained in detail in Melnick et al. (2017), are: a different set of systematics; an improved signal-to-noise (S/N), both in the photometry and in the line widths; a better match between the photometric and spectroscopic apertures; and, most importantly,

* Partly based on data products from observations made with ESO Telescopes at the La Silla Paranal Observatory under ESO programme ID 179.A-2006 and on data products produced by the Cambridge Astronomy Survey Unit on behalf of the VHS and VIDEO consortia.
** Corresponding author; jmelnick@eso.org

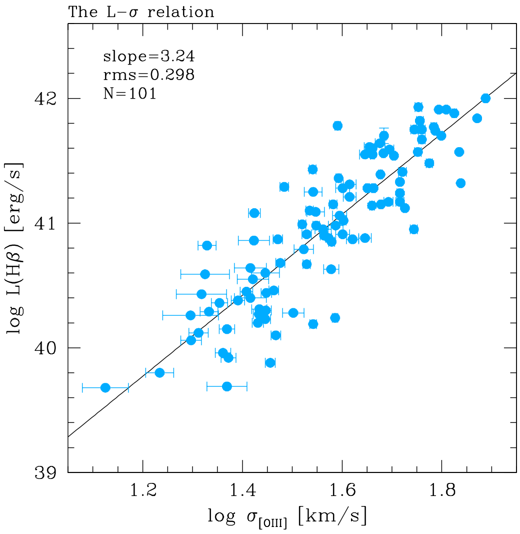

Fig. 1. Observed green $L-\sigma$ relation for HII galaxies using [OIII]5007 velocity dispersions and SDSS Hβ fluxes uncorrected for evolution.

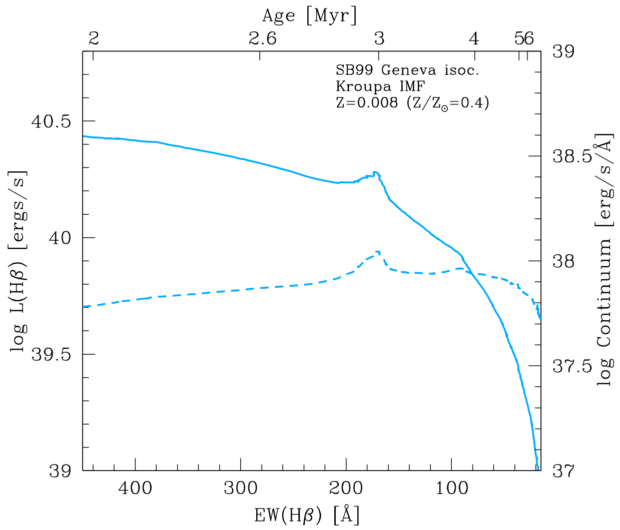

Fig. 2. Starburst99 models showing the evolution of the Hβ and continuum luminosities of a single starburst as a function of the equivalent width of the Hβ emission line. The solid line shows the evolution of the line luminosity and the dashed line shows the evolution of the continuum under the line.

significantly more accurate equivalent widths of Hβ, which are necessary to correct the luminosities for evolutionary effects.

The HII galaxies used to define and calibrate the $L-\sigma$ relation are selected to be very young by including only objects with large equivalent widths (EW(Hβ) > 50 Å), which from Starburst99 (SB99) models (Leitherer et al. 1999) correspond to ages younger than 5–6 million years (Myr). Still, these ages are comparable to the main-sequence lifetimes of the ionizing stars, making it necessary to correct the luminosities for evolutionary effects.

Figure 1 presents the $L-\sigma$ relation derived from these data. Fitting straight lines to data with errors in both variables is complicated and we refer to Melnick et al. (2017) for an in-depth discussion. Since the scatter in the $L-\sigma$ relation is significantly larger than the photometric errors, the parameters from maximum-likelihood solutions are virtually identical to those of standard least-squares techniques, which we use throughout this paper.

As was mentioned above, the galaxies in our sample span a range of ages in which their Hβ luminosities evolve rapidly, so we expect a priori the scatter in the $L-\sigma$ relation to be correlated with age. Figure 2 shows single-burst SB99 models using Geneva isochrones for a metallicity typical for HII galaxies of 40% the solar metallicity. The solid line shows the evolution of the Hβ luminosity as a function of age, parameterized by the equivalent width Hβ, EW(Hβ), and the dashed line shows the evolution of the continuum at the wavelength of Hβ.

These single or "simple" models show that in the first 6 Myrs of evolution the Hβ luminosity decreases by a factor of more than ten, while the continuum increases by about 60%. Most of the galaxies in our sample have Hβ equivalent widths between 50 and 150 Å, so age differences should account for most, if not all, the scatter in the $L-\sigma$ relation. However, in Chávez et al. (2014) and Melnick et al. (2017) we find that the evolutionary corrections derived using SB99 models actually increase the scatter.

In Melnick et al. (2017), we proposed that a likely explanation for this scatter increase is that our chronometer, EW(Hβ), is biased by the contamination of the continuum at Hβ by old and intermediate-age stars. In this paper, we use population synthesis models to evaluate this contamination precisely, and thus correct the observed equivalent widths for contamination by evolved stars.

3. Spectral energy distribution fitting

We used far-ultraviolet (FUV) to mid-infrared (MIR) broadband fluxes from GALEX, SDSS, UKIDSS, VISTA (VHS & VIDEO), and WISE to model the SEDs. To minimize aperture matching effects, we used Petrossian magnitudes, except for GALEX, for which we used model magnitudes. To minimize systematic effects due to different extinction laws, we first corrected the fluxes for foreground Galactic extinction using the values tabulated in SDSS DR13 and a standard Galactic extinction law, and we then applied an internal extinction correction using either a Calzetti or a Gordon extinction law in a subsequent step.

3.1. CIGALE models

We used the package CIGALE (Noll et al. 2009), which offers substantial flexibility for dealing with the various complexities presented by HII galaxies. Full details of our modeling are presented in Telles & Melnick (2018). For the present investigation, we used our Model2 results, for which we fed CIGALE with fluxes corrected for internal extinction using the Balmer decrements (Hα/Hβ) and the reddening law of Gordon et al. (2003) appropriate to the bar of the Small Magellanic Cloud and the 30 Doradus region in the Large Magellanic Cloud, but also allowing CIGALE to make additional corrections (which were almost never necessary or very small). In Model2, we included the WISE W1 (3.7μ) and W2 (4.5μ) bands, but not W3 and W4, where dust emission dominates the fluxes.

We used a special star formation history module kindly provided by M. Bocquien to fit three single bursts: young, intermediate, and old, of a range of ages and durations, which were modeled using BC03 SSP for a Chabrier initial mass function (IMF). Since the nebular continuum is very relevant, particularly in the infrared (IR), we used the nebular module of CIGALE, leaving the ionizing parameter (logU) as a free parameter (−1.5; −2.0; or −3.0). We found that including the WISE W1 and W2

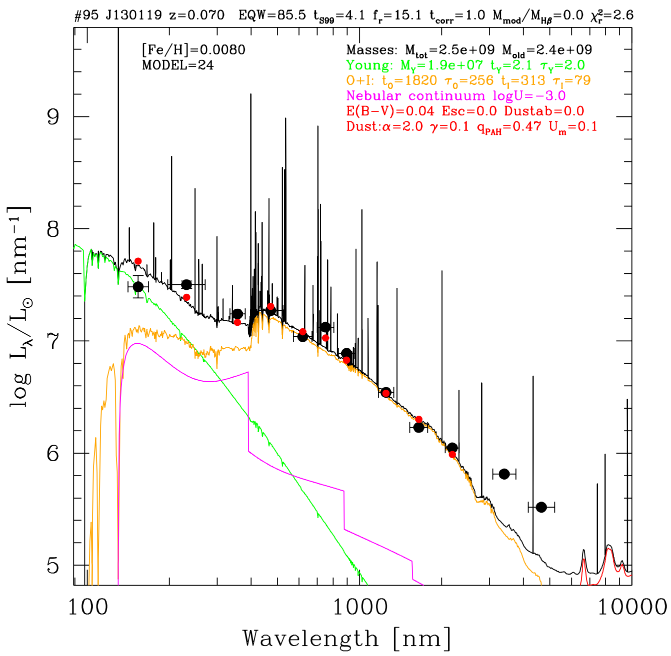

Fig. 3. Examples of spectral energy distribution of two HII galaxies using CIGALE. The black line is the best fit from GIGALE to the observations shown by the black dots. The red dots are the best CIGALE fits convolved with the relevant filter bandpasses. The green line is the young stellar component fit and the orange line the old + intermediate age component. The red line is the dust emission model from Draine & Li (2007) for the parameters indicated in each figure legend; and the magenta line shows the nebular continuum. The top legends show several parameters, including the reduced χ^2 of the solution. Left. CIGALE model fit for J130119. In this case, evolved stars dominate the continuum at most bands, so f_r = 15.1. Right. Same as left, but for J025426, where the young stellar population dominates the continuum at Hβ; thus, f_r = 1.6. The WISE W3 and W4 bands are shown for reference but were not used for the fits (no red dots). More information about these two galaxies is provided in the text.

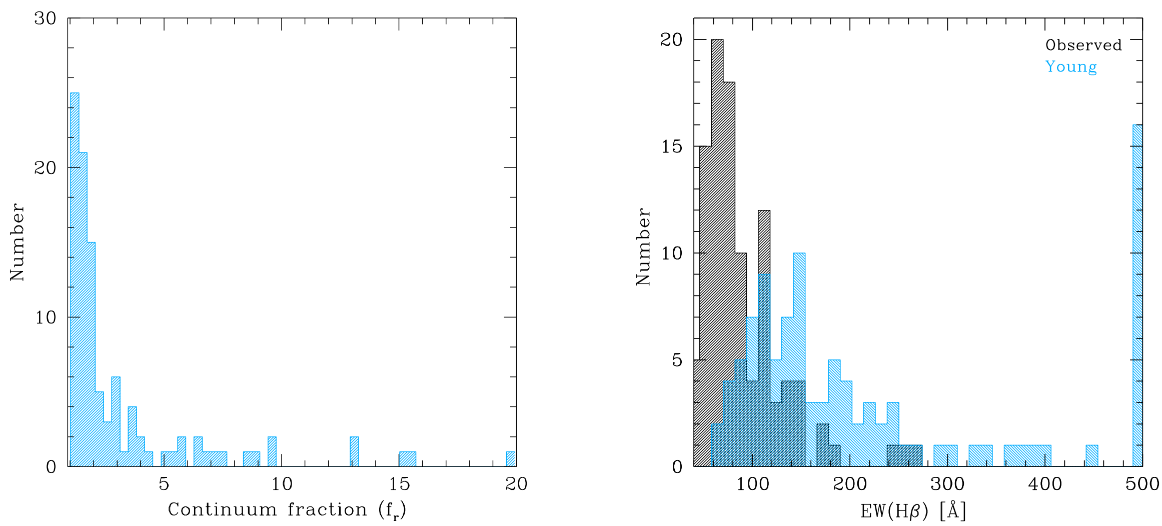

Fig. 4. Distributions of the SED fitting results showing the contamination of the continuum at Hβ by evolved stars. Left. Distribution of the correction factor f_r values given by equation 1. The distribution peaks at f_r = 1.1–1.2, indicating that while all the HII galaxies in this sample have significant underlying old and intermediate-age stellar populations, for most galaxies the effect in EW(Hβ) is seen to be below 50%. Right. Histograms of the distribution of observed EW(Hβ) in black, and corrected (Young) in blue using SED fitting. The distribution of ages [EW(Hβ)] of the young stellar populations is seen to be much flatter than the distribution of observed equivalent widths.

bands increased the stability of the solutions, although at these wavelengths dust emission begins to be important, requiring one to include a dust emission module. We found the best results for the dl2014 (Draine & Li 2007) module, which is the one we used in Model2. The metallicity was allowed to be either $Z = 0.0040$ or $Z = 0.0080$; whichever gives the best fit. Examples of CIGALE fits for two HII galaxies in our sample are presented in Fig. 3.

From the best-fitting spectral decomposition provided by CIGALE (young and old + intermediate age), it is straightforward to deduce the correction to the observed equivalent widths due to contamination by old and intermediate-age stars, which we parameterize as

$$f_r = \frac{\mathrm{EW(H\beta)_{Young}}}{\mathrm{EW(H\beta)_{observed}}}. \quad (1)$$

The distribution of f_r values for our sample is presented in the left-hand plot of Fig. 4, and the observed and corrected (young) distributions of equivalent widths are shown in the right panel. The corrected distribution of ages is now quite different from the observed one.

3.2. The $L - \sigma$ relation revisited

As in Melnick et al. (2017), hereafter Paper I, we used the velocity dispersions from the [OIII]5007 lines, and the Hβ fluxes measured on SDSS spectra, to examine the $L - \sigma$ relation. The extinction corrections were derived from the Balmer decrement (Hα/Hβ) without corrections for underlying absorption. The correlation is presented in Fig. 1 and is the same as what we called the "mixed" $L - \sigma$ relation in that paper.

Table 1 presents the least-squares fit parameters of the $L - \sigma$ relation with and without corrections for evolution, using the equivalent widths as chronometers. The table shows that, contrary to our original expectations, the CIGALE corrections actually increase the scatter of the $L - \sigma$ relation quite substantially. Thus, either our estimations of the "true" equivalent widths are completely off, or other parameters are involved, or both (see Fig. 5).

4. Deconstructing the scatter of the $L - \sigma$ relation

We have seen that naive evolutionary corrections using EW(Hβ) as an evolutionary clock do not explain the scatter of the $L - \sigma$ relation, and that refining our clock through modeling of the underlying stellar continuum does not help. This is puzzling (and disappointing) because the evolutionary corrections are substantial and should stand out over other effects.

4.1. Multiple starbursts

A possible way out of this conundrum is that HII galaxies are actually made of multiple starbursts of different ages. For example, from Fig. 2 it is easy to see that the sum of two starbursts of the same mass, but of different ages, say 2 Myr and 5 Myr, has an Hβ luminosity only 10% larger than the 2 Myr old burst alone, but half the equivalent width. So, if HII galaxies are made of multiple starbursts of different ages, their integrated Hβ equivalent widths may not be a reliable evolutionary clock.

Following Telles et al. (1997), Fernández-Arenas (2018) performed a morphological classification of the HII galaxies in our sample dividing them in two groups: type I for galaxies with disturbed or irregular isophotes; and type II for galaxies with regular isophotes, which were also found to be more compact.

We found that 54 of 103 galaxies in the sample of Fernández-Arenas (2018) are morphological singles (type II), of which 47 are in our sample. Figure 6 shows the observed $L - \sigma$ relation for these 47 galaxies; the parameters of the relation corrected for evolution using the equivalent widths of the starburst component are shown in Table 2.

Table 2 shows that correcting for evolution using the equivalent widths of Hβ with or without corrections for contamination by evolved stars does not reduce the scatter of the $L - \sigma$ relation for single starbursts. On the contrary, as was the case for the full sample, these corrections actually increase the scatter quite significantly.

However, not all HII galaxies classified as single on the basis of optical morphology have Gaussian [OIII] profiles. In fact, selecting only single galaxies with Gaussian profiles (determined by visual inspection) leaves only 22 galaxies, which is too few to allow further analysis.

Table 1. Evolutionary corrections for the full sample.

	Without age corrections	Corrected using observed EW(Hβ)	Corrected using CIGALE EW(Hβ)
Slope	3.24 ± 0.18	3.50 ± 0.21	3.40 ± 0.23
rms	0.298	0.337	0.372

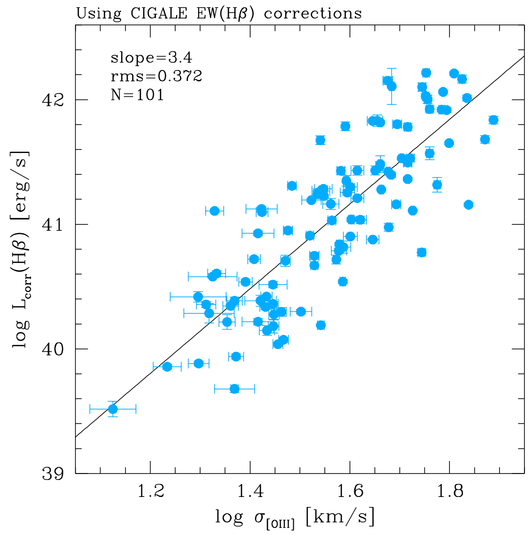

Fig. 5. $L - \sigma$ relation with the luminosities corrected for evolution, and the equivalent widths of Hβ corrected for contamination by evolved stars by our CIGALE models.

Table 2. Evolutionary corrections for starbursts of single morphology.

	Without age corrections	Corrected using observed EW(Hβ)	Corrected using CIGALE EW(Hβ)
Slope	3.68 ± 0.25	4.03 ± 0.27	4.11 ± 0.30
rms	0.271	0.298	0.326

4.2. Other parameters

Of the various observables tested by Chávez et al. (2014) (and later Fernández-Arenas (2018)) as possible additional parameters of the $L - \sigma$ relation, the size of the objects, measured by the Petrossian radii in u'-band SDSS images (R_u), gave the strongest signal. R_u was chosen because contamination by nebular lines and continuum is minimal in the u' band. However, as is shown in Fig. 3, contamination by the nebular continuum and/or by evolved stars is dominant for several objects in our sample.

Table 3 shows the results of repeating the analysis of Chávez et al. (2014) using the radii of Fernández-Arenas (2018), but our velocity dispersions and luminosities and the corresponding evolutionary corrections. The table shows the results of fitting

$$\log L(\mathrm{H}\beta) = c_0 + c_1 \times \log \sigma_{[\mathrm{OIII}]} + c_2 \times \log R_u \qquad (2)$$

using standard LSQ techniques.

Table 3 shows that including the radius as a second parameter leads, at face value, to a significant reduction in the scatter,

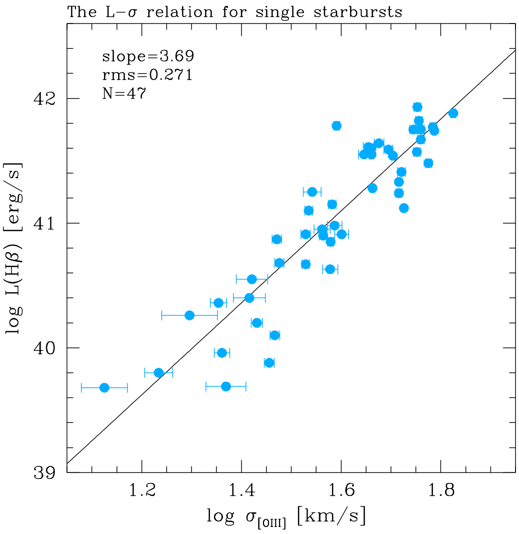

Fig. 6. $L-\sigma$ relation for HII galaxies classified as single starbursts on the basis of morphology.

Table 3. Radius as a second parameter.

Parameter	Without age corrections	Fluxes corrected using observed EW(Hβ)	Fluxes corrected using CIGALE EW(Hβ)
c_0	34.96 ± 0.25	34.70 ± 0.27	33.84 ± 0.29
c_1	2.12 ± 0.21	2.11 ± 0.22	2.42 ± 0.24
c_2	1.00 ± 0.12	1.21 ± 0.13	1.24 ± 0.14
rms	0.223	0.242	0.261

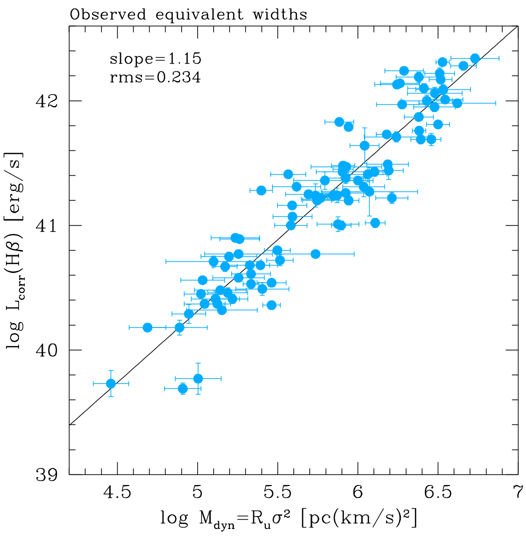

Fig. 7. Relation between Hβ luminosity corrected for evolution using the observed equivalent widths, and the dynamical mass defined as $M_{\rm dyn} = R_u\sigma^2$ in the text. The line shows a least-squares fit of parameters shown in the figure labels.

and that the $L-\sigma$ relation appears actually to be a correlation between the integrated Hβ luminosity of HII galaxies and $R_u\sigma^2$, reminiscent of some sort of dynamical mass. This can be visualized in Fig. 7, where the Hβ luminosity is plotted against this "dynamical" mass, $M_{\rm dyn} = R_u\sigma^2$

This correlation brings us back to the arcane discussion of whether HII galaxies (and their local siblings, the Giant HII

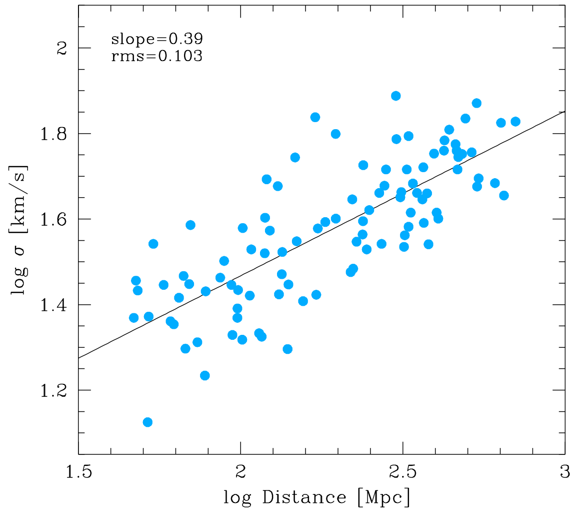

Fig. 8. Malmquist bias in our flux-limited sample of HII galaxies produces a correlation between the distance-independent parameter, σ, and distance.

Regions (GHRs)) are self-gravitating balls of ionized gas (see Terlevich et al. 2018 for a recent discussion and a comprehensive list of references). We know that the velocity dispersions of GHRs, measured by the width of their emission lines, are not due to the motions of ionized blobs of gas moving in the gravitational potential of these systems, but rather the result of the superposition of multiple stellar-wind (actually cluster-wind) driven bubbles of ionized gas (Melnick et al. 2021). Since GHR and HII galaxies follow the same $L-\sigma$ relation, it would be very surprising if their velocity dispersions had a different physical origin, which would also invalidate the use of GHR as zero point calibrators of the $L-\sigma$ distance indicator. Our strong view is that in both classes of objects the gas motions are driven by stellar winds and that the tight correlation between L(Hβ) and $R_u\sigma^2$ is not due to gravity but has a different explanation: Malmquist bias.

Figure 8 plots σ as a function of distance, D. The least-squares fit shown by the line has the functional form $\sigma \sim D^{0.39}$, so $R_u\sigma^2$ goes as $D^{1.8}$, and in log-log we expect a tight correlation between L(Hβ) (or $M_{\rm young}$) and $R_u\sigma^2$ of the slope close to unity, as we observe. The ranges spanned by the Hβ fluxes and angular sizes of HII galaxies are much smaller than their range of distances.

Every time we deal with log-log plots of a slope very close to unity, where some parameter (in our case the distance) appears in both axes to a similar power, we must ask ourselves whether we have a true correlation or a "Stork" diagram[1].

It is easy to show, by scrambling the (angular) radii, or by simply replacing R_u with the distance, that Fig. 7 is a classical Stork diagram. With our present sample, it is not possible to establish whether there is any correlation between luminosity and starburst dimensions, even if such a correlation could be envisaged if the sizes correlated with the cluster mass.

Moreover, our CIGALE models show that the contribution of nebular emission and evolved stars to the light in the SDSS u' band varies significantly, while about 80% of the galaxies in our sample have multiple components. In practice, therefore, R_u measures something different from one galaxy to the next. This

[1] The logarithm of the number of Storks per capita in European cities correlates perfectly with the logarithm of the number of births per capita; Storks bring babies.

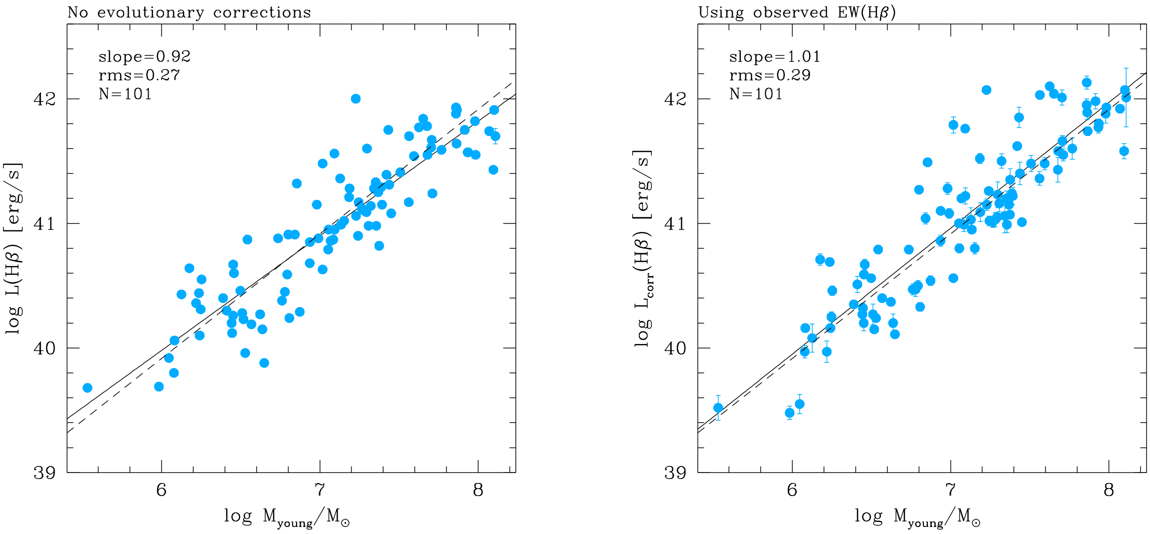

Fig. 9. Relation between photometric mass of young stars ($M_{\rm young}$) from CIGALE SED fits and the observed Hβ luminosity. Left. In this case, the observed Hβ luminosity is not corrected for evolution. Right. Same as left, but with Hβ luminosity corrected for evolution using the observed EW(Hβ). The solid lines shows a least-squares fits to the data; the dashed line plots the predictions of SB99 models. As is discussed in the text, this is a classical Stork diagram: the logarithm of the distance appears in both axes.

supports our strong conclusion that HII galaxies are not self-gravitating balls of ionized gas and that the supersonic velocities inferred by the widths of the emission lines are due to a superposition of a large number of wind-driven bubbles of gas.

5. Discussion

5.1. Whether EW(Hβ) is a reasonable evolutionary chronometer

We have seen that the observed EW(Hβ) works better as an evolutionary chronometer than the equivalent width corrected for contamination by evolved stars from SED fits, although neither adequately explains the scatter of the $L-\sigma$ relation. We argued that the uncorrected EW(Hβ) works better because the majority of the HII galaxies in our sample contain multiple starburst components, but we have not demonstrated that our clock actually works.

From our previous work modeling a sample of 2234 high-excitation SDSS HII galaxies (Telles & Melnick 2018), we know that the observed EW(Hβ) work reasonably well in that sample, a subset of the parent population of 4200 SDSS high excitation HII galaxies with EW(Hβ) > 50 Å, used in Chávez et al. (2014) to select the 101 galaxies in our $L-\sigma$ sample. The number is reduced to 2234 selecting objects with published ultraviolet to MIR photometry.

In Telles & Melnick (2018), we found that the mass of young stars, $M_{\rm young}$, derived from SED fitting with CIGALE, correlates extremely well with Hβ luminosity. Of course, this is a classical log-log Stork diagram (the square of the distance appears on both axes), but the interesting result is that the scatter is reduced to just the observational errors when the luminosities are corrected for evolution using the observed EW(Hβ) and SB99 models.

Figure 9 shows the relation between $M_{\rm young}$ and L(Hβ) for the 101 HII galaxies in our [OIII] $L-\sigma$ sample. In the left-hand panel, the luminosities are uncorrected for evolution. The right-hand panel shows the luminosities corrected for evolution, as in Telles & Melnick (2018). Although at first glance the correlation appears to be tighter that the panel on the left, the scatter is actually (slightly) worse. The dashed line plots the luminosities predicted by SB99 models (at the mean age of the sample) for the $M_{\rm young}$ masses from CIGALE. The excellent consistency with the observed luminosities (solid line) shows that it is probably okay to use SB99 models in the present context, and that we can trust our CIGALE masses (but see below).

If that is the case, however, the question arises of why the EW(Hβ) corrections do not work as well as they did for the 'parent' sample. Closer inspection of the right panel shows that the scatter is dominated by just a few objects. In fact, there are ten objects with deviations of more than a factor of three from the best fit line that have a common feature: their luminosities are dominated by the old + intermediate age component, not by the young stars. Figure 3 shows the SED of one of these objects, J130119.

The answer to the title of this section is, therefore: yes, but the $L-\sigma$ sample contains many objects with SEDs dominated by old + intermediate age stars that require large corrections. Removing such objects improves the indicator substantially but at a high cost: removing luminous HII galaxies (which contain multiple starbursts and tend to have low equivalent widths) makes it more difficult to find suitable HII galaxies at high redshifts.

5.2. Whether the turbulence of the ionized gas evolves together with L(Hβ)

The turbulence of the ionized gas could be evolving together with the luminosity, due, for example, to the onset of Type-Ic supernovae. Figure 10 plots the velocity dispersion, σ, as a function of the mass of young stars from the CIGALE models. The points are color-coded according to the CIGALE continuum correction factor, f_r.

The correlation between σ and $M_{\rm young}$ is weaker than expected. Part of the scatter is due to the outliers discussed in the previous section, but not all. Most of the outliers in this plot do not show any identifiable peculiarities. Incidentally, the σ–$M_{\rm young}$ relation is also noisy in the parent sample, but with a significantly flatter slope (0.118 ± 0.008 versus 0.214 ± 0.017 shown in the figure). Malmquist bias may explain the difference in slope, but we have not investigated this any further.

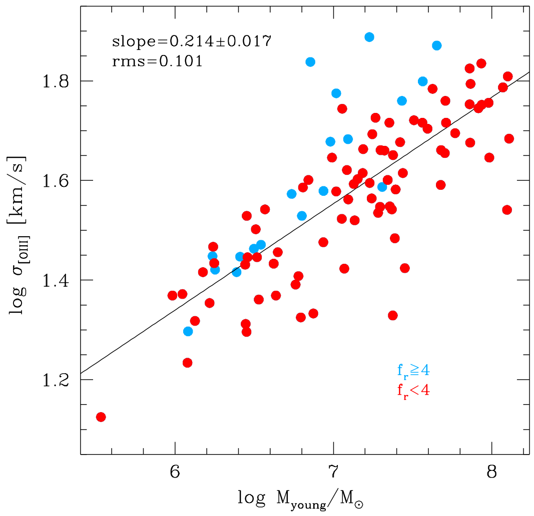

Fig. 10. Relation between photometric mass of young stars ($M_{\rm young}$) from CIGALE SED fits and the equivalent width of Hβ. The colors code objects with dominant old + intermediate stellar populations that have large continuum corrections, f_r.

The answer to the title of this section is, therefore: no. With the exception of the outliers, we do not see any correlation between the scatter in the relation between σ and $M_{\rm young}$ and EW(Hβ).

6. Conclusion: The scatter of the $L-\sigma$ relation

Several factors determine the scatter of the relation:

1. Outliers. A few peculiar objects have an inordinate effect on the scatter. The optical-IR fluxes of these objects are dominated by old + intermediate stars, whereas by definition the SEDs of HII galaxies should be dominated by the young stellar component.
2. Evolution. The range of ages spanned by the galaxies in the $L-\sigma$ sample implies that evolutionary corrections to the Hβ luminosities are important. However, about 80% of the HII galaxies in our sample appear to have multiple starburst components, seen either on direct images or from multiple bumps in the integrated [OIII] profiles. Multiplicity reduces the efficacy of EW(Hβ) as an evolutionary chronometer so, although we do detect the effects of evolution, with the available tools and observations it is not possible to normalize the luminosities to some fiducial age.
3. The turbulence of the ionized gas measured by the widths of the emission lines is only loosely correlated with the mass of the ionizing clusters. The velocity dispersion scales as $\sigma \sim M_{\rm young}^{1/5}$, indicating that the transformation of stellar winds into the cluster winds that ultimately inflate the bubbles of ionized gas is a highly dissipative process in which most of the kinetic energy of the stellar winds is thermalized at high temperatures (Melnick et al. 2021). This suggests that the mass and the age of the ionizing stars may not be the only parameters the govern the physics of the $L-\sigma$ relation.
4. Given that the observed scatter of the relation is not very sensitive to evolutionary corrections, which should be large, it is unlikely that subtler effects, such as changes in the IMF, or the metallicity of the stars, contribute significantly to the scatter.
5. Observations of the starburst cluster 30 Doradus (see Crowther (2019) for a recent review) indicate that HII galaxies may contain tens to hundreds of supermassive stars ($M > 150\,{\rm M}_\odot$) that are not included in either SB99 or CIGALE models. Our analysis of the evolution of HII galaxies, therefore, may be incomplete, in particular for the youngest objects.

With the presently available sample, it does not appear possible to reduce the scatter of the $L-\sigma$ relation below ~0.3 dex. It may be possible to improve the precision of the relation as a distance indicator by selecting galaxies with substantially larger equivalent widths. As it stands, the $L-\sigma$ relation does not seem to be precise enough to be used as a cosmological distance indicator. Not all HII galaxies can be used as standard candles.

Acknowledgements. We are grateful to Denis Burgarella, the father of CIGALE, and to Mederic Bocquien for guiding us through our first steps with the code and answering numerous questions. Mederic kindly wrote the special module to fit three stellar populations that we used in this work. JM acknowledges support from a CNPq *Ciência sem Fronteiras* grant at the Observatorio Nacional in Rio de Janeiro, and the hospitality of ON as a PVE visitor. Funding for the SDSS and SDSS-II has been provided by the Alfred P. Sloan Foundation, the Participating Institutions, the National Science Foundation, the U.S. Department of Energy, the National Aeronautics and Space Administration, the Japanese Monbukagakusho, the Max Planck Society, and the Higher Education Funding Council for England. The SDSS Web Site is http://www.sdss.org/. The SDSS is managed by the Astrophysical Research Consortium for the Participating Institutions. The Participating Institutions are the American Museum of Natural History, Astrophysical Institute Potsdam, University of Basel, University of Cambridge, Case Western Reserve University, University of Chicago, Drexel University, Fermilab, the Institute for Advanced Study, the Japan Participation Group, Johns Hopkins University, the Joint Institute for Nuclear Astrophysics, the Kavli Institute for Particle Astrophysics and Cosmology, the Korean Scientist Group, the Chinese Academy of Sciences (LAMOST), Los Alamos National Laboratory, the Max-Planck-Institute for Astronomy (MPIA), the Max-Planck-Institute for Astrophysics (MPA), New Mexico State University, Ohio State University, University of Pittsburgh, University of Portsmouth, Princeton University, the United States Naval Observatory, and the University of Washington. The entire GALEX Team gratefully acknowledges NASA's support for construction, operation, and science analysis for the GALEX mission, developed in corporation with the Centre National d'Etudes Spatiales of France and the Korean Ministry of Science and Technology. We acknowledge the dedicated team of engineers, technicians, and administrative staff from JPL/Caltech, Orbital Sciences Corporation, University of California, Berkeley, Laboratoire d'Astrophysique Marseille, and the other institutions who made this mission possible. We make use of the UKIRT InfraRed Deep Sky Surveys (UKIDSS) from the WFCAM Science Archive (WSA) generated by the Wide Field Camera (WFCAM) on the United Kingdom Infrared Telescope (UKIRT). We gratefully acknowledge use of data from the ESO Public Survey programme ID 179.B-2004 taken with the VISTA telescope, data products from CASU and VSA archive operated by WFAU. This publication makes use of data products from the Wide-field Infrared Survey Explorer, which is a joint project of the University of California, Los Angeles, and the Jet Propulsion Laboratory/California Institute of Technology, funded by the National Aeronautics and Space Administration.

References

Chávez, R., Terlevich, R., Terlevich, E., et al. 2014, MNRAS, 442, 3565
Chávez, R., Terlevich, R., Terlevich, E., et al. 2024, ArXiv e-prints [arXiv:2404.16261]
Crowther, P. A. 2019, Galaxies, 7, 88
Draine, B. T., & Li, A. 2007, ApJ, 657, 810
Fernández-Arenas, D. 2018, Ph.D. Thesis, INAOEP, Mexico
González-Morán, A. L., Chávez, R., Terlevich, E., et al. 2021, MNRAS, 505, 1441
Gordon, K. D., Clayton, G. C., Misselt, K. A., Landolt, A. U., & Wolff, M. J. 2003, ApJ, 594, 279
Leitherer, C., Schaerer, D., Goldader, J. D., et al. 1999, ApJS, 123, 3
Melnick, J., Telles, E., Bordalo, V., et al. 2017, A&A, 599, A76
Melnick, J., Tenorio-Tagle, G., & Telles, E. 2021, A&A, 649, A175
Noll, S., Burgarella, D., Giovannoli, E., et al. 2009, A&A, 507, 1793
Telles, E., & Melnick, J. 2018, A&A, 615, A55
Telles, E., Melnick, J., & Terlevich, R. 1997, MNRAS, 288, 78
Terlevich, E., Fernández-Arenas, D., Terlevich, R., et al. 2018, MNRAS, 481, 268